

Experimental analysis of the impact of selected laser processing parameters on wettability and surface free energy of EN AW-2024 and EN AW-5083 aluminum alloys

Barbara Ewa Ciecńska^{1*} , Jacek Mucha² 

¹ Department of Manufacturing Processes and Production Engineering, Faculty of Mechanical Engineering and Aeronautics, Rzeszow University of Technology, Powstańców Warszawy 12, Rzeszów, Poland

² Department of Mechanical Engineering, Faculty of Mechanical Engineering and Aeronautics, Rzeszow University of Technology, Powstańców Warszawy 12, Rzeszów, Poland

* Corresponding author's e-mail: barbara.ciecinska@prz.edu.pl

ABSTRACT

Surface wettability is a useful feature in many coating or bonding technological operations, where adhesion conditions play a crucial role for the efficiency of the technology and the durability of the produced parts. The article presents an analysis of different ways of creating surface wettability. Based on experimental studies conducted on EN AW-2024 and EN AW-5083 aluminum alloys samples, the effects of laser processing performed with different parameters of a 500 W pulsed laser are shown in the context of the achieved wettability of the sheet surface. The effects of laser treatment were related to the delivery condition (rolling) and compared with typical technological operation of surface preparing used for aluminum alloys: grinding, manual sandpaper processing, sandblasting and chemical treatment (allodyning). The aim of this study is to analyze the energy properties of aluminum alloys. Surface free energy calculations were carried out based on measurements made with two liquids, water and diiodomethane. Attention was paid to the reproducibility of surface effects, or lack thereof, resulting from the nature of the used treatment. Advantages and disadvantages were pointed out for the described methods of preparing the sheet surface for coating (painting, gluing). The possibility of improving surface wettability more effectively by laser treatment compared to other traditional methods was emphasized. Finally, it was found that, in the case of EN AW-2024 alloy, treatment with the selected laser at a scanning speed of $V_s = 2000$ mm/s and pulse frequency $f_i = 15$ kHz allowed a surface energy of $\gamma_s = 85.8$ mJ/m² to be obtained, while a maximum of $\gamma_s = 64.4$ mJ/m² (after grinding) was obtained after conventional treatment. In the case of EN AW-5083 alloy, the best energy results were obtained after laser treatment with scanning speed $V_s = 2000$ mm/s and pulse frequency $f_i = 10$ kHz, when free surface energy $\gamma_s = 75.5$ mJ/m² was obtained, while the conventionally prepared surface was characterized by energy $\gamma_s = 53.9$ mJ/m² (after sandblasting).

Keywords: laser treatment, wettability, surface free energy, aluminum alloy EN AW-2024 and EN AW-5083.

INTRODUCTION

Aluminum alloys, used extensively in automotive and aerospace applications, among others, require a certain surface condition, e.g. cleanliness, geometric structure. In many technological assembly operations, improvement of the surface condition is needed, an example being adhesive operations and the need to improve adhesion conditions. This is usually done by abrasive or

chemical treatment. During abrasive treatment, e.g. grinding, different types of tools are used: bonded abrasive wheels, paper-backed abrasive papers or non-woven abrasives. The surface can also be sandblasted. The use of this type of treatment allows the removal of unnecessary oxide layers and structuring of the surface [1].

Chemical treatment, on the other hand, which comes in three basic varieties: acid bath etching, anodizing in sulphuric acid and anodizing in

chromium acid, involves etching the surface in acid or alkaline baths [2, 3]. Their purpose can be to produce a durable oxide layer, characterized by a certain roughness, porosity and also aesthetic value in use due to the yellow or green color of this layer.

However, the aforementioned methods, considered as conventional, are troublesome due to the waste load (e.g. used abrasive tools, contaminated chemical bath solutions), atmospheric dust emissions (e.g. during grinding and sandblasting), or the need to use a number of chemicals that are harmful to human health and the environment (as during electroplating). Currently, there is an intensive search for environmentally friendly methods, and the possibility of eliminating so-called wet chemistry in surface preparation processes before further processing [4 ÷ 6].

Wettability is an important characteristic of the surface layer of materials and has been widely described and studied in the past several decades due to its important roles in fundamental research and practical application [7, 8]. The issue is being addressed in physics, chemistry, materials engineering and biotechnology due to its usefulness in both low and high wettability contexts [2]. Low wettability is desirable in the context of self-cleaning, antifogging, oil-water separation, or anti-corrosion properties [9, 10]. In contrast, in applications such as printing, surface coating, painting, lubrication and gluing, high wettability is essential [6, 11]. Wettability can be measured by various methods, but ultimately can be used to determine the energy state of a surface expressed by the determined surface free energy (SFE) value. The more energetically active a surface is, the higher the SFE value is [12, 13].

In order to activate the surface, the previously mentioned conventional methods are used, but due to their disadvantages, alternative methods such as ozone, plasma and laser treatment are implemented. For example, the paper [2] reported the results of ozonation of EN AW-1050A aluminum and EN AW-2017A aluminum alloy. In the case of EN AW-1050A, the possibility of improving the surface free energy γ_s to about 55 ÷ 62 mJ/m² depending on the ozone concentration was indicated (while the γ_s of the surface before ozonation was about 50 mJ/m²). Tests conducted on EN AW-2017A aluminum alloy also show the possibility of surface activation from about 6 mJ/m² before treatment, to about 19 mJ/m² after ozonation. In addition, polymers are subjected to

ozonation. For example, the authors of the paper [14] ozonated polyamide (PA) and improved the surface free energy. Tests conducted on sandpaper-prepared and ozonated material indicate that the surface energy can be improved from 51 to 55 mJ/m². According to [15], on the other hand, the effects of plasma treatment are interesting because of the significant reduction in the water wetting angle. Plasma treatment of polyethylene terephthalate (PET) allowed to achieve θ_w equal from 50° even to about 18°, while low density polyethylene (LDPE) – from 31° to 10°, depending on the number of cycles. Laser treatment in the context of surface activation is presented, for example, in the work [16], where a carbon fiber reinforced polymer/plastic composite was laser treated and a surface free energy in the range of about 58 ÷ 62 mJ/m² was obtained, while the raw surface of the composite had γ_s equal to about 52 mJ/m² and the sandblasted surface 48 mJ/m².

This paper presents the results of an experimental study to investigate the effect of fiber laser treatment of the surfaces of selected aluminum alloys on their wettability. The surfaces of rolled samples subjected to sandblasting, grinding, chemical treatment and laser treatment were examined. The positive effects of laser surface activation and the possibility of replacing conventional methods with modern, reproducible and environmentally safe laser processing were indicated.

MATERIALS AND METHODS

Materials

Sheets 1 mm thick of EN AW-2024 aluminum alloy in the technological condition T351 and EN AW-5083 alloy in the technological condition H111 were used for the experimental tests. The chemical composition and basic mechanical properties of the alloys are given in Table 1 and 2.

Samples measuring $15.0 \pm 0.2 \times 100$ mm were cut along the rolling direction from the sheets.

Sample preparation

For the comparative analysis related to the wettability of the tested materials, samples were prepared whose surfaces were subjected to respectively:

- sandblasting (variant S) – samples cut from sheet metal were subjected to abrasive blasting in an ejector chamber using fine-grained

Table 1. Chemical composition and properties of tested alloys [17]

Alloy	Element (maximum percentage by weight, %)									
	Mg	Mn	Fe	Si	Cu	Zn	Cr	Ti	Zr+Ti	Others
EN AW-2024	1.8	0.9	0.5	0.5	4.9	0.25	0.1	0.15	0.2	0.15
EN AW-5083	4.9	1.0	0.4	0.4	0.1	0.25	0.25	0.15	-	0.15

Table 2. Mechanical properties of tested alloys [17]

Heat-treated condition	Brinell hardness, HB	Young's modulus E , GPa	Poisson's ratio ν	Yield strength $R_{p0.2}$ (min.), MPa	Tensile strength R_m (min.), MPa	Elongation after fracture $A_{50\%}$, %
EN AW-2024						
T351	120	74	0.33	290	435	20
EN AW-5083						
H111	75	71	0.33	125	275	12

F280-type electro corundum with an average size of $45 \pm 4 \mu\text{m}$, for 3 seconds at a nozzle operating pressure of 0.2 MPa, nozzle at a 45° angle. The samples were then rinsed with demineralized water at room temperature and dried in air ($22 \pm 2 \text{ }^\circ\text{C}$);

- grinding (variant G) – the surface of the samples was ground with a flap wheel with an abrasive grit gradation of P120 at a longitudinal feed rate of 115 mm/min;
- allodyning (variant A) – the samples were sequentially degreased with acetone and immersed in a 30% aqueous nitric acid solution for about 2 min. The samples were then immersed for 1 h in a $50 \text{ }^\circ\text{C}$ solution that contained potassium dichromate $\text{K}_2\text{Cr}_2\text{O}_7$ (23g), concentrated phosphoric acid H_3PO_4 (180 g), sodium fluoride NaF (2.5 g) and water (to a volume of 2 l). The samples were green with a tinge of yellow when removed. After removal from the bath, the samples were rinsed with running water and then immersed for approximately 30 s in an aqueous 0.1 percent chromic acid anhydride solution heated to $50 \text{ }^\circ\text{C}$ in order to seal and fix the produced allodin coating. Finally, the samples were rinsed in water and dried at ambient temperature ($22 \pm 2 \text{ }^\circ\text{C}$) [18, 19].
- laser machining (variant L1-L9) – concentrated energy beam machining was performed using a pulsed fiber laser (SLCR Germany), with a nominal power of 500 W, an energy density of $7 \div 33 \text{ J/cm}^2$, a pulse duration of 10 ns and a wavelength of 1070 nm. The laser head was mounted in a special holder in the spindle of a conventional universal milling machine with turned off the spindle rotation function. The

laser head only provided beam movement in one plane, so surface processing was ensured with a constant movement of the machine table of 115 mm/min. on which the samples were placed (Fig. 1).

Table 3 summarizes the laser parameters for the adopted processing variants. In order to demonstrate the effect of surface treatment on the change in wettability, samples with a non-mechanically modified surface (as-rolled) were also prepared for testing, their surfaces washed with aliphatic hydrocarbon-based agent C_nH_{2n} to degrease and remove contaminants (variant R in the experiment).

The surfaces of the tested samples had a defined surface roughness, which was measured in two perpendicular directions with three repetitions

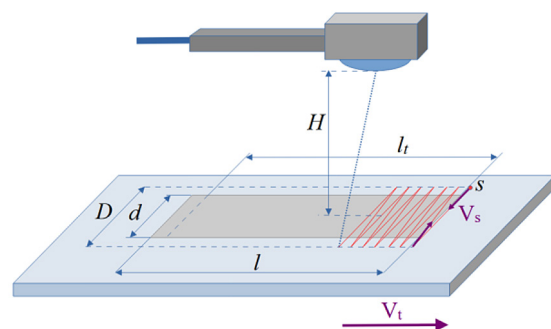


Figure 1. Laser processing scheme, where: V_s – laser beam scanning speed, mm/s; V_t – movement speed of the machine table; mm/min; D – scanning width, mm; H – distance of the lens from the sample, mm; d – sample width, mm; l – sample length, mm; l_t – length of the laser working field, s – start point of laser beam impact

Table 3. Laser processing parameters

Option designation	Impulse frequency, f , kHz	Scanning speed, V_s , mm/s
L1	10	2000
L2		4000
L3		6000
L4	15	2000
L5		4000
L6		6000
L7	20	2000
L8		4000
L9		6000

on a measuring length of 4 mm using a Surtronic 25 profilometer (Taylor Hobson, UK) together with TalyProfile Silver software. The average values of the Ra parameter are given in Table 4.

Method of determining surface free energy

In interfacial areas, such as solid-liquid, solid-vapor and vapor-liquid, atoms belonging to each phase are subjected to a different system of forces than atoms deep within the phase [9, 20]. Atoms in the depth of the phase are surrounded on all sides by atoms of the same type, and it is assumed that a balanced system of attraction and repulsion forces acts on each such atom, between that atom and a neighboring atom. Atoms in the interfacial region or at the phase boundary are on the one hand attracted by the neighboring atoms of their phase and on the other hand are attracted by atoms from the neighboring phase. They are in an asymmetric force field. When the forces of attraction towards one phase are greater, the atoms migrate deeper into that phase until they reach equilibrium. The equilibrium state, which was first described in 1805 by T. Young, is described,

among other things, by a thermodynamic function such as the surface free energy [9, 21]. The Owens-Wendt indirect method [22] was used to determine the surface free energy, on available the measurement instrumentation. It assumes that the surface free energy has two components: dispersive and polar. To determine these components, surface contact angle measurements were made with two liquids with different characteristics [23]. One liquid, had a large value of the dispersive component γ_L^d and a small value of the polar component γ_L^p , and the other vice versa, according to the principles given in [24]. Water and diiodomethane were used in the measurements, with the values of the polar and dispersive components given in Table 5.

By applying a drop of first and then a drop of the second measuring liquid to the test material, a system is created for which the energy balance for the equilibrium point of the three phases can be represented as in Figure 2. This balance is expressed by Young’s equation [7]:

$$\gamma_{SV} = \gamma_{SL} + \gamma_{LV} \cos\theta \tag{1}$$

where: γ_{SV} – surface free energy of the material, γ_{SL} – surface tension at the material-liquid interface, γ_{LV} – surface tension at the measuring liquid-air interface (gas), θ – contact angle of a given liquid.

In the method proposed by Owens-Wendt, the surface free energy γ_s of the material under test is the sum of the dispersive and polar components [2, 7]:

$$\gamma_s = \gamma_s^d + \gamma_s^p \tag{2}$$

where: γ_s^d – dispersive component SFE of material, γ_s^p – polar component SFE of material.

Finally, these components can be determined from the relationships [2]:

Table 4. Average surface roughness value of the samples Ra , μm

Material	Type of preparatory treatment				
	Rolling (R)	Sandblasting (S)	Grinding (B)	Allodyning (A)	Laser (L1 + L9)
EN AW-2024	0.294	0.592	7.615	0.474	0.580 ÷ 0.720
EN AW-5083	0.478	0.585	3.150	0.245	0.450 ÷ 0.535

Table 5. Values of surface free energy and its components of polar and dispersive measuring fluids [24]

Liquid	Surface free energy γ_L , mJ/m^2	Dispersive component γ_L^d , mJ/m^2	Polar component γ_L^p , mJ/m^2
Water	72.8	21.8	51
Diiodomethane	50.8	48.5	2.3

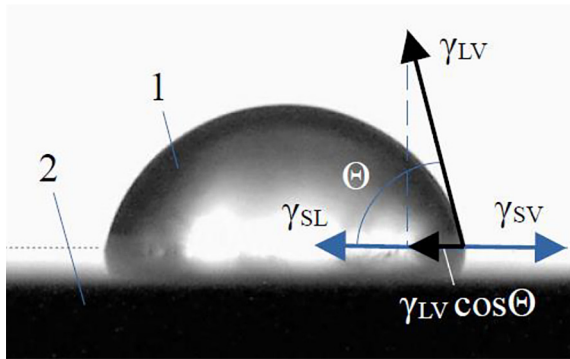


Figure 2. Graphical interpretation of Young's Equation: 1 – measuring droplet, 2 – test substrate

$$(\gamma_s^d)^{0.5} = \frac{\gamma_d(\cos\theta_d + 1) - \frac{\gamma_d^p}{\gamma_w} \gamma_w(\cos\theta_w + 1)}{2 \left(\sqrt{\gamma_d^d} - \sqrt{\gamma_d^p \gamma_w^d} \right)} \quad (3)$$

$$(\gamma_s^p)^{0.5} = \frac{\gamma_w(\cos\theta_w + 1) - 2\sqrt{\gamma_s^d \gamma_w^d}}{2\sqrt{\gamma_w^p}} \quad (4)$$

where: θ_w – water contact angle, θ_d – diiodomethane contact angle.

Contact angle θ was measured with a PG-3 goniometer (FIBRO System AB, Sweden), distilled water and diiodomethane, applying 10 drops of 4 μ l to each sample. The results obtained, shown as an example in Figure 3, allowed the calculation of SFE.

RESULTS AND DISCUSSION

Wettability measurements were carried out on samples from both aluminum alloys, with surfaces modified by laser beam, by grinding, sandblasting, allodyned and surfaces without any treatment (post-rolled condition). Ten drops each of the liquid in question were applied to the prepared samples of the test materials. Measurements were performed in triplicate.

Table 6 shows the average values of the contact angles measured on the surfaces of the tested materials. Using the relationships (2÷4) given in the Owens-Wendt method, the surface free energy values of the alloys and the polar and dispersive components were calculated. The results of the calculations are given in Table 7 and 8.

In the pursuit of favorable surface wettability, it is important to obtain as flat a measuring liquid droplet as possible, which at the same time means a small contact angle.

The wettability of a surface is influenced by many factors, including its state of geometric structure, as well as the method of processing [25]. The geometric structure of the surfaces of the tested alloys varied. After sandblasting, grinding and allodyning, the values of the parameter Ra for the EN AW-2024 alloy were slightly higher than the Ra of the EN AW-5083 alloy, and the surface energy γ_s had a similar relationship. After

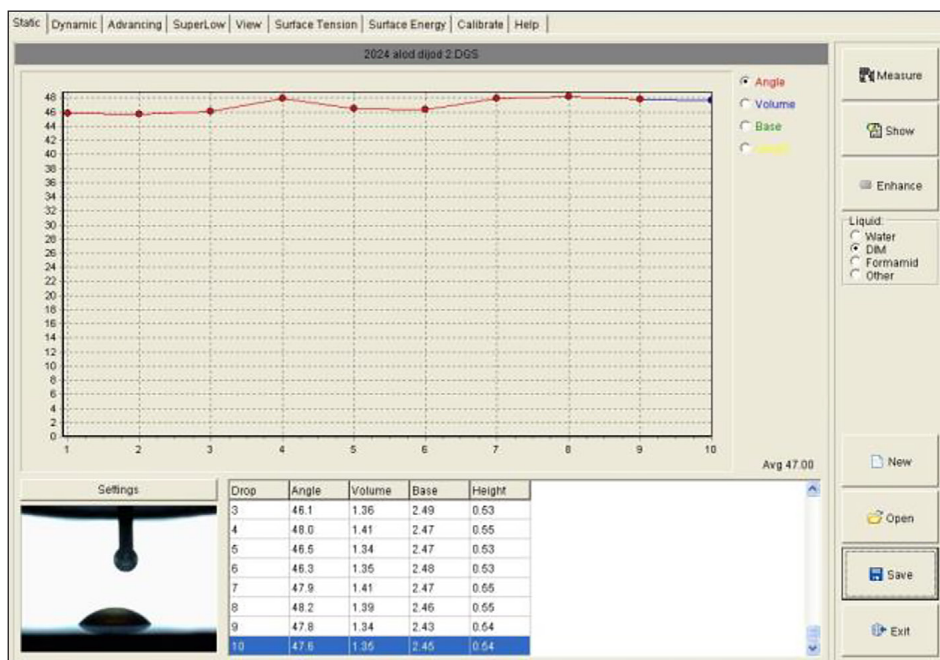


Figure 3. Example of a software window with results of contact angle measurements with a selected measuring liquid

Table 6. Average contact angle (θ)

Surface modification option	EN AW-2024		EN AW-5083	
	Water θ_w , °	Diiodomethane θ_d , °	Water θ_w , °	Diiodomethane θ_d , °
L1	36.8	8.1	20.9	42.0
L2	13.6	10.4	24.8	39.3
L3	7.9	13.8	27.3	39.2
L4	13.1	13.3	29.7	40.4
L5	17.1	20.9	26.4	39.5
L6	30.0	34.8	47.7	36.9
L7	7.9	33.8	46.8	39.8
L8	16.6	37.1	51.2	39.6
L9	19.5	38.9	54.3	45.1
Ground (G)	51.8	33.0	66.0	46.1
Sandblasted (S)	38.2	61.3	63.7	46.0
Allodyned (A)	48.7	45.5	105.6	35.5
Rolled (R)	83.9	48.1	86.6	34.5

Table 7. Surface free energy (γ_s), polar component (γ_s^p) and dispersive component (γ_s^d) of EN AW-2024 alloy

Surface modification option	Surface free energy (SFE) γ_s , mJ/m ²	Polar component of SFE γ_s^p , mJ/m ²	Dispersive component of SFE γ_s^d , mJ/m ²
L1	77.1	26.8	50.3
L2	85.8	35.8	50.0
L3	84.5	35.1	49.4
L4	84.6	35.1	49.5
L5	82.3	34.7	47.6
L6	78.6	31.7	42.5
L7	80.9	38.0	42.9
L8	78.4	35.9	41.5
L9	74.7	37.0	40.7
Ground (G)	64.4	21.2	43.2
Sandblasted (S)	62.5	32.6	29.8
Allodyned (A)	52.4	11.3	41.1
Rolled (R)	47.8	5.2	42.6

laser treatment of EN AW-2024 alloy, a wider range of roughness and higher Ra values were obtained compared to EN AW-5083. However, treatment with concentrated energy beam resulted in different energy effects. In contrast, after rolling, the EN AW-2024 alloy had twice the roughness Ra of the EN AW-5083 alloy, and the surface energy γ_s was higher. This variation depending on the treatment and differences in surface activation are shown in Figures 4 and 5.

Analyzing the results for EN AW-2024 alloy (Fig. 4a), it can be seen that each type of treatment resulted in improved wettability. The water contact angle of the rolled surface was $\theta_w = 83.9^\circ$,

while the traditionally used methods of modifying the surface reduced it. The most effective in this respect was sandblasting (variant S), after which $\theta_w = 38.2^\circ$. Allodyning and grinding gave slightly worse results, with $\theta_w = 48.7^\circ$ (variant A) and $\theta_w = 51.8^\circ$ (variant G), respectively. Laser treatment resulted in an increase in wettability by a greater value as for variants A and S.

During laser beam processing at 10 kHz with the lowest applied speed $V_s = 2000$ mm/s, the angle θ_w was 36.8° . Increasing the speed to 4000 mm/s reduced θ_w to 13.6° , while at $V_s = 6000$ mm/s θ_w was 7.9° . In contrast, increasing the pulse frequency from 10 kHz to 15 kHz increased θ_w

Table 8. Surface free energy (γ_s), polar component (γ_s^p) and dispersive component (γ_s^d) of EN AW-5083 alloy

Surface modification option	Surface free energy (SFE) γ_s^t , mJ/m ²	Polar component of SFE γ_s^p , mJ/m ²	Dispersive component of SFE γ_s^d , mJ/m ²
L1	75.5	36.2	39.2
L2	74.9	34.4	40.5
L3	73.0	33.4	40.5
L4	72.9	32.5	40.4
L5	72.2	31.8	40.4
L6	65.2	23.6	41.6
L7	64.7	23.4	41.3
L8	62.5	22.2	40.3
L9	59.0	21.2	37.8
Ground (G)	52.7	15.4	37.3
Sandblasted (S)	53.9	16.6	37.3
Allodyned (A)	40.7	39.6	1.1
Rolled (R)	48.0	5.4	42.6

from 13.1° to 30.0°, respectively, as the scanning speed increased (variants L4 ÷ L6), compared to a minimum value of 7.9°. A further increase in pulse frequency to 20 kHz enabled improved water wettability, with θ_w angles ranging from 7.9° to 19.9°, but also increasing with increasing scanning speed (variants L7 ÷ L9).

Variants L3 and L7 had the same minimum water wettability. When the wettability of EN AW-2024 alloy was tested with diiodomethane (Fig. 4b), it was found that more favorable surface wettability was obtained compared to the rolled condition and after treatment with the S and A variants, using a laser. The maximum

diiodomethane contact angle θ_d had a value slightly lower than allodyning and of 45.1°, while after allodyning θ_d was 45.5°. However, in contrast to the wettability tested with water, laser treatment from variants L6 to L9 gave worse results than grinding (G), where θ_d was 33.0°. Variants L1÷L5, however, allow for improved wettability with diiodomethane. Machining with a pulse frequency of 10 kHz and a scanning speed of 2000 mm/s (variant L1) gives the best result, the angle θ_d was 8.1° and this was the minimum value. The angle θ_d increased with increasing scanning speed and pulse frequency; for variant L5, more favorable than grinding, it was 20.9°.

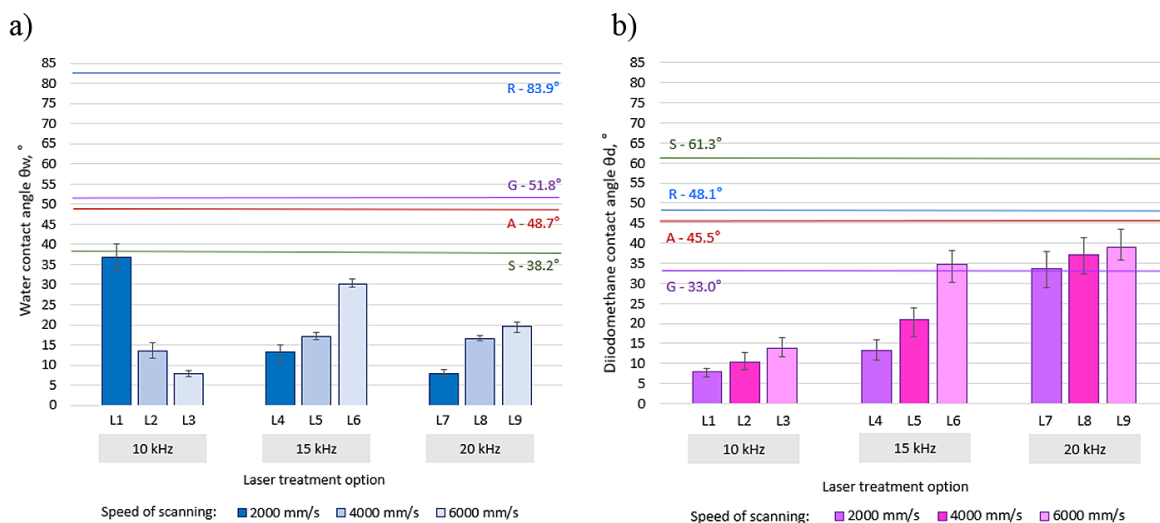


Figure 4. Results of contact angle measurement of EN AW-2024 alloy: a) water measurement (θ_w), b) diiodomethane measurement (θ_d); L1 ÷ L9 – laser treatment options, S – sandblasting, A – allodyning, G – grinding, R – rolling

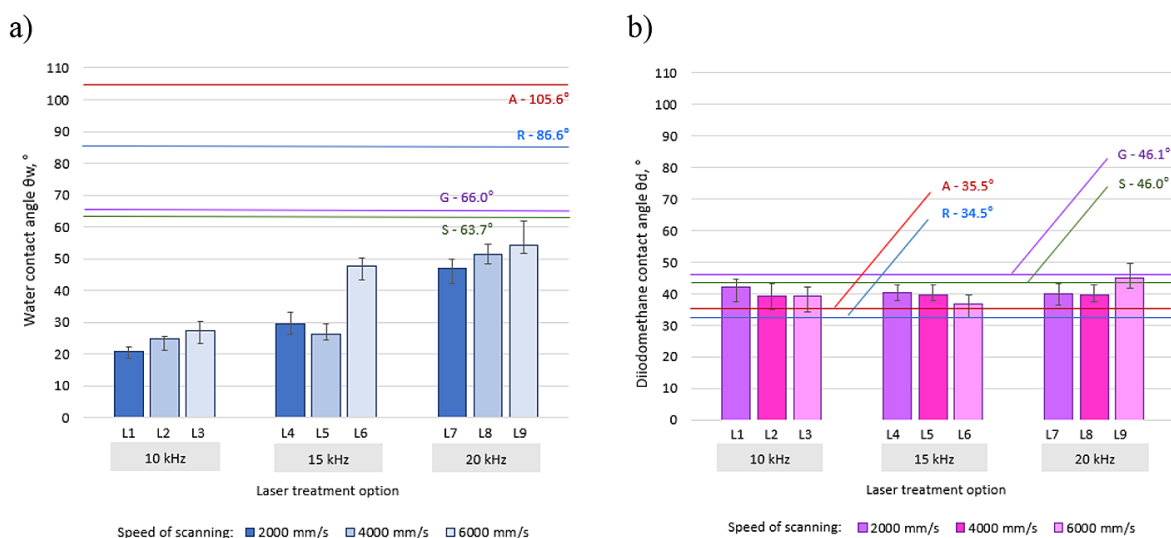


Figure 5. Results of contact angle measurement of EN AW-5083 alloy: a) water measurement (θ_w), b) diiodomethane measurement (θ_d); L1 ÷ L9 – laser treatment options, S – sandblasting, A – allodyning, G – grinding, R – rolling

Analyzing the obtained results of the contact angle measurement for EN AW-5083 alloy (Fig. 5a), it can be concluded that the wettability tested with water is favorable after laser treatment compared to variants S, G and A, as well as rolling R. The best, among variants S, G and A, for surface modification turned out to be sandblasting S (similarly to EN AW-2024). On the other hand, after laser treatment, the best result was obtained for a frequency of 10 kHz and a speed of 2000 mm/s (L1), where θ_w was 20.9°.

This angle increased with increasing pulse frequency and scanning speed, up to a value of 54.3°. However, the most favorable treatment is with a frequency of 10 kHz and a change in speed from 2000 mm/s to 4000 and 6000 mm/s, where the angle θ_w is low (24.8° for the L2 variant and 27.3° for the L3 variant, respectively). On the other hand, when the wettability of the laser-beam-modified surfaces was tested with diiodomethane (Fig. 5b), it was found to be similar to the values obtained after conventional treatment, i.e. after allodyning, $\theta_d = 35.5^\circ$ was obtained, while in the rolled state θ_d was 34.5°. After laser treatment, the angle θ_d varied between 36.9° and 45.1°. These values were only more favorable in comparison with the abrasive treatment of the analyzed alloy, when after sandblasting θ_d was 46.0°, while after grinding it was 46.1°.

By determining the contact angle SFE from measurements, it can be concluded for EN AW-2024 alloy (Fig. 6a) that laser treatment in all

variants of the tested processing parameters increased surface adhesion. A maximum SFE value of 85.8 mJ/m² can be indicated for the L3 variant, which represents treatment at a pulse frequency of 10 kHz and a speed of scanning of 6000 mm/s, while the best conventional treatment variant was grinding (SFE was 64.4 mJ/m²).

In the case of EN AW-5083 alloy (Fig. 6b), on the other hand, a downward trend is apparent, starting from a maximum value of 75.5 mJ/m² in the L1 treatment variant, gradually to a value of 59.0 mJ/m² in the L9 variant. However, a laser with suitable parameters can produce an energetically more favorable state compared to the other investigated surface modification methods. Sandblasting was then the best option, followed by a surface energy of 62 mJ/m². All treatments, with the sole exception of the allodyning of EN AW-5083 alloy, resulted in a better SFE value compared to the as-rolled condition. The analysis of the SFE components, polar (γ_L^p) and dispersive (γ_L^d), is helpful in selecting the best option. From the point of view of adhesion of the binder to the substrate, a higher value of the polar component is desirable. In the case of EN AW-2024 alloy (Fig. 7a), the highest value after laser treatment was recorded for the L7 variant, where it was 38.0 mJ/m². Comparing to the other used treatments, this was higher than the best sandblasting, when it was 32.6 mJ/m².

In the case of the EN AW-5083 material under study (Fig. 7b), the polar component was most

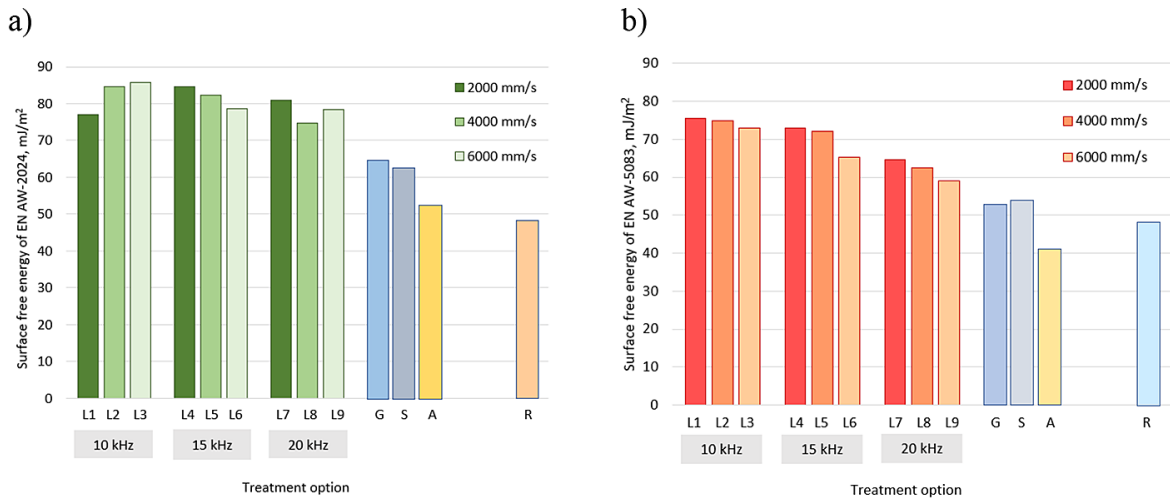


Figure 6. Surface free energy (SFE): a) EN AW-2024, b) EN AW-5083; L1 ÷ L9 – laser treatment options, S – sandblasting, A – allodyning, G – grinding, R – rolling

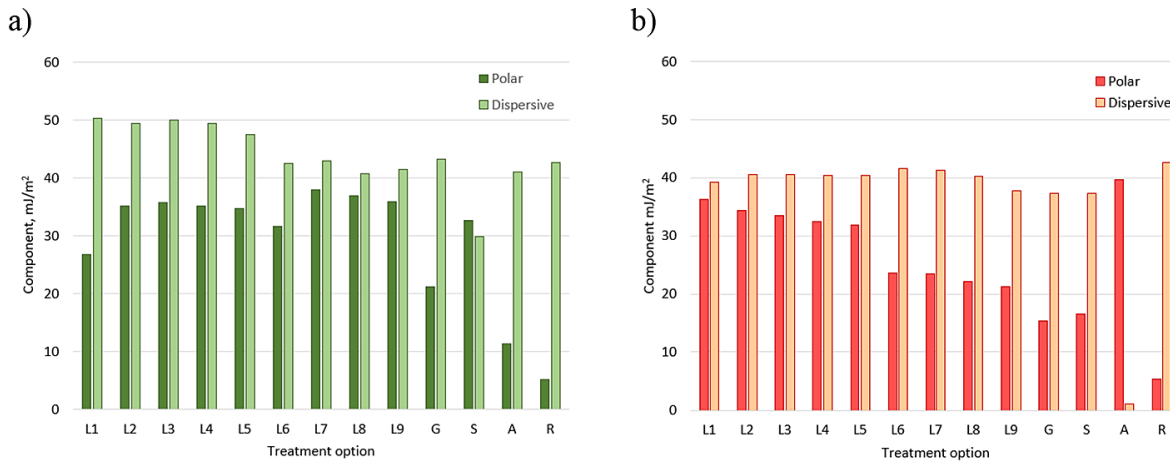


Figure 7. Polar and dispersive components of SFE of alloys: a) EN AW-2024, b) EN AW-5083; L1 ÷ L9 – laser treatment options, S – sandblasting, A – allodyning, G – grinding, R – rolling

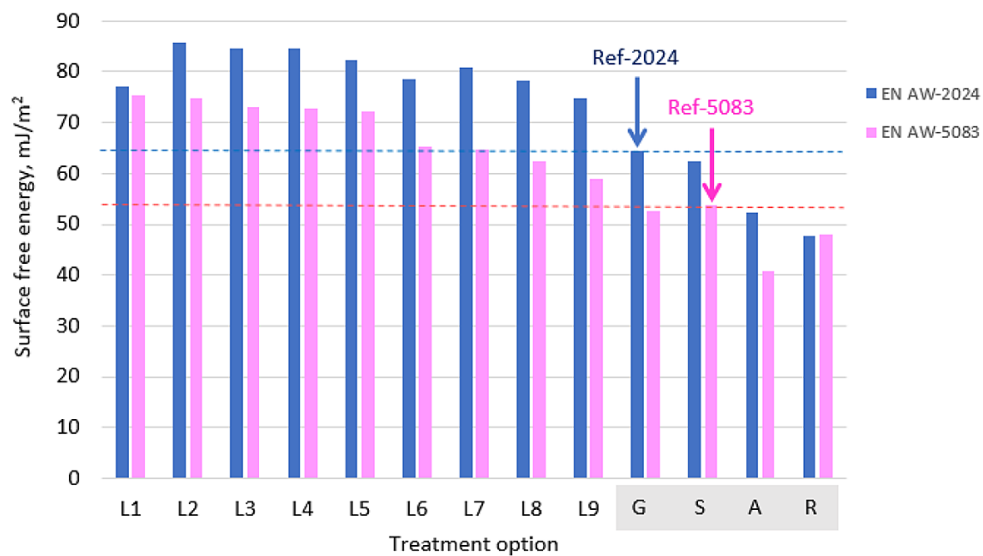


Figure 8. Comparison of the average SFE value of EN AW-2024 and EN AW-5083 alloys; L1÷L9 – laser treatment options, S – sandblasting, A – allodyning, G – grinding, R – rolling

favorable in the L1 variant and its value decreased progressively up to the value obtained in the L9 treatment variant. This is a trend analogous to the surface energy of the analyzed material. Thus, the choice of the best option from the point of view of the SFE simultaneously implies the best option from the point of view of the polar component. However, in the case of this alloy, the highest polar component was obtained after allodyning.

For the tested materials, the conventional treatment variant for which the SFE value is the highest was determined and respectively designated Ref-2024 and Ref-5083 (Fig. 8). Relative to this value, the percentage increase in SFE after laser treatment was determined (Fig. 9).

Analyzing the effect of scanning speed (V_s) on the resulting SFE values at the assumed pulse frequency (Fig. 10), it can be seen that, for EN AW-2024 at 10 kHz, the SFE increases with machining acceleration, i.e. from 77.1 mJ/m² for 2000 mm/s to 84.8 mJ/m² for 6000 mm/s, while machining at 15 kHz causes the SFE to decrease with increasing speed (from 84.6 mJ/m² at 2000

mm/s to 78.6 mJ/m² at 6000 mm/s). A similar phenomenon of a slight decrease in SFE can be observed when machining at 20 kHz, when it drops from 80.9 mJ/m² at 2000 mm/s to 74.7 mJ/m² for 6000 mm/s.

In the case of EN AW-5083 alloy at 10 kHz, fairly similar SFE values were obtained regardless of the velocity: 75.5 mJ/m² ($V_s = 2000$ mm/s), 74.9 mJ/m² ($V_s = 4000$ mm/s) and 73.0 mJ/m² ($V_s = 6000$ mm/s). Processing at 15 and 20 kHz results in the highest SFE value for 6000 mm/s. The least favorable result was obtained for a velocity of 4000 mm/s at both pulse frequencies.

Despite the adopted identical treatments of the two selected aluminum alloys, differences in the degree of surface activation and the value of the surface free energy γ_s were experimentally demonstrated. The processes occurring during the heating of different materials with a laser beam are presented in the work [26]. Surface treatment with a laser beam is accompanied by a very rapid and microlocal increase in the temperature of the material, the melted particles transfer heat to the

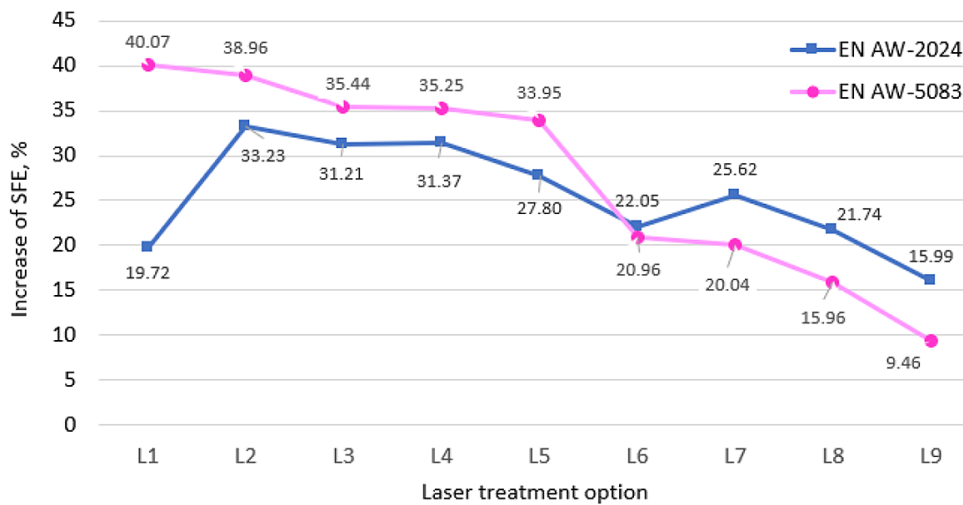


Figure 9. Percentage increase in SFE of tested aluminum alloys

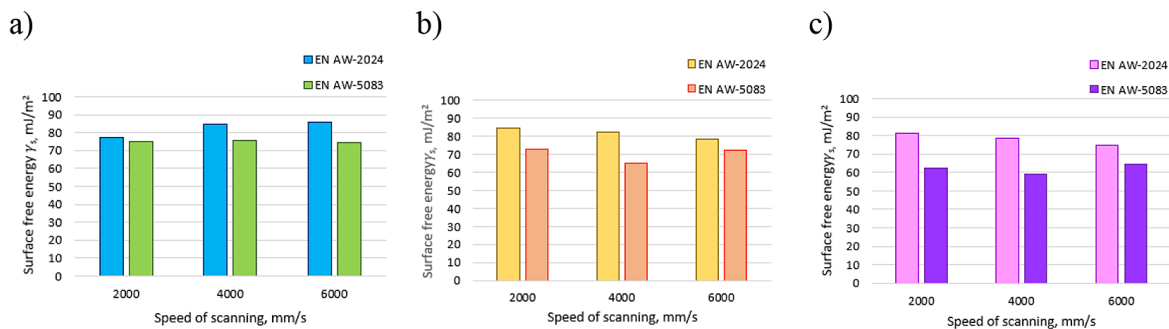


Figure 10. Effect of scanning speed on mean SFE at frequency: a) 10 kHz, b) 15 kHz, c) 20 kHz

environment and the substrate at high speed. In such a process, the cooling rates of the metal can reach up to 10^{11} K/s. An altered metallographic structure is constituted in the top layer. An altered metallographic structure is constituted in the top layer. The cooling rate is influenced by the processing time, the radiation power density, and the volume of molten material [27, 28]. Technological parameters of the laser beam surface treatment process also affect the change in the value of the components of the residual stresses in the near-surface layer of the material [29, 30]. The state of residual stress in the material's surface layer affects the constitution of the material's surface tension. Aluminum alloys EN AW-2024 and EN AW-5083 are characterized by different solidus temperatures and proportions of alloying additives, hence the surface effects vary.

CONCLUSIONS

Different surface energy states can be obtained by using different preparatory treatments. By using a surface modification method other than chemical or mechanical treatment, i.e. pulsed laser beam modification, higher surface free energy values can be obtained. Therefore, this method of surface treatment is a promising alternative and can also bring advantages in the area of production organization, due to easy automation, computerization possibilities and robotization of the treatment process. The main conclusions from the study were:

The interaction frequency of the laser pulse significantly influences the change in the contact angle (θ) of a given liquid. In the case of treating the surface of EN AW-5083 alloy with a laser beam at $f_i = 10$ kHz, the smallest contact angle values were obtained ($\theta_w = 20.9^\circ$). Increasing f_i by 100% resulted in an increase of the angle θ_w by approximately 124% ($\theta_w = 46.8^\circ$ at 20 kHz). Wetting conditions are also affected by the speed at which the surface is scanned with the laser beam. Increasing the speed of laser beam travel (V_s) from 2000 mm/min to 6000 mm/s (200% increase) at 10 kHz resulted in an increase in angle of approximately 30% (θ_w from 20.9° to 27.3°).

A similar trend of increasing water contact angle with increasing speed was observed for 15 and 20 kHz. Thus, in order to obtain favourable water wetting conditions, the EN AW-5083 alloy

should be processed with the selected laser at a lower frequency and lower scanning speed.

For the surface of EN AW-2024 alloy samples, a slightly different trend was obtained. At a scanning speed of $V_s = 2000$ mm/s, there was a favourable trend. Increasing the frequency f_i from 10 kHz to 15 kHz resulted in a decrease in the angle θ_w of approximately 64.4%, while increasing the frequency f_i from 10 kHz to 20 kHz resulted in a decrease in the angle θ_w of approximately 78.5%. The most favourable wetting conditions for EN AW-2024 alloy occurred at $V_s = 2000$ mm/s, so this material should be processed with the selected laser at the highest frequency and lowest scanning speed.

The use of diiodomethane, a liquid with different properties to water, for the analysis of surface wettability by measuring the angle θ , resulted in an increasing trend of the angle θ_d as the frequency f_i and speed V_s were increased in the context of the EN AW-2024 alloy. Treatment with a frequency $f_i = 10$ kHz and speed $V_s = 2000$ mm/s resulted in an angle $\theta_d = 8.1^\circ$, while increasing the pulse frequency and scanning speed increased θ_d to a value of 38.9° . Thus, if it is necessary under technological conditions to prepare a surface with characteristics favourable for wetting with a liquid with diiodomethane properties, laser processing with the lowest speed and frequency is advantageous.

In the case of EN AW-5083 alloy, similar values for the angle θ_d were obtained in all laser treatment variants. In the best case ($f_i = 15$ kHz, $V_s = 6000$ mm/s), θ_d was about 6.5% higher than after rolling, and about 3.8% higher than after chemical treatment. The surface condition after rolling for the analysed materials was characterised by a mean roughness parameter of $Ra = 0.294 \mu\text{m}$ (EN AW-2024) and $Ra = 0.478 \mu\text{m}$ (EN AW-5083).

Treating the surface of EN AW-2024 alloy with a laser beam increased the roughness by about 2 ÷ 2.5 times (an increase of about 140 ÷ 145%), and the surface free energy γ_s increased from about 56% (in the L9 variant) to about 80% (in the L3 variant).

Laser treatment of EN AW-5083 alloy also produced a favourable result, although the roughness Ra compared to rolling changed slightly, by a maximum of about 12%. The surface free energy γ_s , however, increased significantly, from 23% in the L9 variant to about 57% in the L1 variant. The maximum value of the surface free energy γ_s

on the surface of EN AW-2024 alloy depending on the scanning speed V_s was obtained: for $V_s = 2000$ mm/s at $f_i = 15$ kHz, for $V_s = 4000$ mm/s at $f_i = 10$ kHz, and for $V_s = 6000$ mm/s at $f_i = 10$ kHz.

In contrast, on the EN AW-5083 alloy surface, the maximum value of γ_s was obtained for three values of scanning speed V_s : 2000 mm/s, 4000 mm/s and 6000 mm/s with a frequency $f_i = 10$ kHz.

The above differences in the free energy values obtained for the two different aluminium alloys were mainly influenced by the surface roughness, chemical composition and technological state of the material.

Acknowledgments

The research leading to these results has received funding from the commissioned task entitled “VIA CARPATIA Universities of Technology Network named after the President of the Republic of Poland Lech Kaczyński”, under the special purpose grant from the Minister of Science, contract no. MEIN/2022/DPI/2578 action entitled “In the neighborhood – inter-university research internships and study visits”.

REFERENCES

- Oczos K.E., Kawalec A. *Kształtowanie metali lekkich* (in English: Light metal forming), PWN, Warszawa, 2012.
- Kłonica M., Kuczmaszewski J. Ozonization as a method of energetic activation of surface layer of selected construction materials in adhesive joint operations (in Polish: Ozonowanie jako metoda aktywowania warstwy wierzchniej materiałów konstrukcyjnych w operacjach klejenia). *Technologia i Automatykacja Montażu*, 2/2011, 38–46.
- Ciecińska B., Mucha J., Bąk Ł. Analysis of the effect of surface preparation of aluminum alloy sheets on the load-bearing capacity and failure energy of an epoxy-bonded adhesive joint. *Materials*. 2024, 17(9), 1948.
- Kłonica M., Chatys R., Blumbergs I. Strength Analysis of Lap Joints in Aerospace Structural Materials. *Advances in Science and Technology. Research Journal*, 2022, 16(6), 147–155. <https://doi.org/10.12913/22998624/156071>
- Ciecińska B. Using lasers as safe alternatives for adhesive bonding. emerging research and opportunities. IGI Global, Hershey, 2020.
- Belaud V., Valette S., Stremdoerfer G., Bigerelle M., Benayoun S. Wettability versus roughness: Multi-scales approach, *Tribology International*, 2015, 82, Part B, 343–349, <https://doi.org/10.1016/j.triboint.2014.07.002>
- Zhang P., Wang S., Wang S., Jiang L. Superwetting Surfaces under Different Media: Effects of Surface Topography on Wettability. *Small*, 2015, 11: 1939–1946. <https://doi.org/10.1002/sml.201401869>
- Slepickova Kasalkova N., Slepicka P., Kolska Z., Svorcik V. Wettability and Other Surface Properties of Modified Polymers. IntechOpen Ltd. London UK, 2015, 12, 323–356.
- Jothi Prakash C.G., Prasanth R. Approaches to design a surface with tunable wettability: a review on surface properties. *J Mater Sci* 2021, 56, 108–135. <https://doi.org/10.1007/s10853-020-05116-1>
- Law K.Y., Zhao H. Determination of solid surface tension by contact angle. In: *Surface Wetting*. Springer, Cham. 2016, https://doi.org/10.1007/978-3-319-25214-8_7
- Kuznetsov G.V., Orlova E.G., Feoktistov D.V., Islamova A.G., Zhuikov A.V. Droplet spreading and wettability of abrasive processed aluminum alloy surfaces. *Metals and Materials International*, 2020, 26, 46–55. <https://doi.org/10.1007/s12540-019-00310-6>
- Kung, C.H., Sow P.K., Zahiri B., Mérida W. Assessment and interpretation of surface wettability based on sessile droplet contact angle measurement: challenges and opportunities. *Advanced Materials Interfaces*, 2019, 6(18), 1900839. <https://doi.org/10.1002/admi.201900839>
- Cwikel D., Zhao Q., Liu C., Su X., Marmur A. Comparing contact angle measurements and surface tension assessments of solid surfaces. *Langmuir* 2010, 26(19), 15289–15294 <https://doi.org/10.1021/la1020252>
- Kłonica M. Application of the ozonation process for shaping the energy properties of the surface layer of polymer construction materials. *Journal of Ecological Engineering*, 2022, 23(2).
- Sant’Ana P.L., Bortoleto J.R., Drrant S.F. Contact Angle and Wettability of Commercial Polymers after Plasma Treatment. *LJP*, 2022, 22, 13–33.
- Kłonica M., Kubit A., Perłowski R., Bielawski R., Woś S. Selected methods of modifying the surface layer of a carbon composite. *Advances in Science and Technology. Research Journal*, 2024, 18(1). <https://doi.org/10.12913/22998624/183101>
- EN 573-3:2019 Aluminium and aluminium alloys - Chemical composition and form of wrought products - Part 3: Chemical composition and form of products.
- PN-EN 2437 Chromate conversion coatings (yellow) for aluminium and aluminium alloys.
- PN-EN 4729:2017:10 Aerospace series. Trivalent chromium based chemical conversion coatings for aluminium and aluminium alloys.

20. Marmur A., Volpe C., Siboni S., Amirfazli A., Drelich J. Contact angles and wettability: towards common and accurate terminology. *Surface Innovations*, 2017, 5(1), 3–8. <https://doi.org/10.1680/jsuin.17.00002>
21. Żenkiewicz M. Methods for the calculation of surface free energy of solids. *Journal of Achievements of Materials and Manufacturing Engineering*, 2007, 24(1), 137–145.
22. Owens D.K., Wendt R.C. Estimation of the surface free energy of polymers. *Journal of Applied Polymer Science*, 1969, 13(8), 1741–1747. <https://doi.org/10.1002/app.1969.070130815>
23. Malaki M., Fadaei Tehrani A., Niroumand B., Gupta M. Wettability in metal matrix composites. *Metals*, 2021, 11(7), 1034. <https://doi.org/10.3390/met11071034>
24. Żenkiewicz M. Adhesion and modification of the surface layer of macromolecular plastics. WNT, Warszawa, 2000.
25. Rudawska A., Zaleski K., Miturska I., Skoczylas A. Effect of the application of different surface treatment methods on the strength of titanium alloy sheet adhesive lap joints. *Materials*, 2019, 12(24), 4173. <https://doi.org/10.3390/ma12244173>
26. Dowden J. (Ed), *The theory of laser materials processing. Heat and Mass Transfer in Modern Technology*. Springer, 2009.
27. Azari, S., Papini, M., & Spelt, J.K. Effect of surface roughness on the performance of adhesive joints under static and cyclic loading. *The Journal of Adhesion*, 2010, 86(7), 742–764, <https://doi.org/10.1080/00218464.2010.482430>
28. Bhowmik A., Yang Y., Zhou W., Chew Y., Bi G., On the heterogeneous cooling rates in laser-clad Al-50Si alloy, *Surface and Coatings Technology*, 2021, 408, 126780. <https://doi.org/10.1016/j.surfcoat.2020.126780>
29. Skoczylas A., Zaleski K., Ciecieląg K., Matuszak J. Study on the surface layer properties of magnesium alloys after impulse shot peening. *The International Journal of Advanced Manufacturing Technology* 2024, 134, 191–204. <https://doi.org/10.1007/s00170-024-14099-1>
30. Matuszak J., Zaleski K., Skoczylas A., Ciecieląg K., Kęćik K. Influence of semi – random and regular shot peening on selected surface layer properties of aluminum alloy. *Materials*. 2021, 14, 7620. <https://doi.org/10.3390/ma14247620>